Article

Photoluminescent Microbit Inscripion inside Dielectric Crystals by Ultrashort Laser Pulses for Archival Applications

Sergey Kudryashov *, Pavel Danilov, Nikita Smirnov, Evgeny Kuzmin, Alexey Rupasov, Roman Khmelnitskii, George Krasin, Irina Mushkarina, Alexey Gorevoy

Posted Date: 11 May 2023

doi: 10.20944/preprints202305.0799.v1

Keywords: fluorides; diamond; ultrashort-pulse laser; direct laser inscription; photoluminescent microbits; vacancy clusters

Article

Photoluminescent microbit inscripion inside dielectric crystals by ultrashort laser pulses for archival applications

Sergey Kudryashov *, Pavel Danilov, Nikita Smirnov, Evgeny Kuzmin, Alexey Rupasov, Roman Khmelnitskii, George Krasin, Irina Mushkarina and Alexey Gorevoy

Lebedev Physical Institute, 119991 Moscow, Russia; danilovpa@lebedev.ru (PD); smirnovna@lebedev.ru (NS); e.kuzmin@lebedev.ru (EK); rupasovan@lebedev.ru (AR); khmelnitskyra@lebedev.ru (RK); krasingk@lebedev.ru (GK); i.mushkarina@lebedev.ru (IM); a.gorevoy@lebedev.ru (AG)

* Correspondence: kudryashovsi@lebedev.ru

Abstract: Inscription of embedded photoluminescent microbits inside a bulk natural diamond, LiF and CaF_2 crystals was performed in sub-filamentation (geometrical focusing) regime by 525-nm 0.2-ps laser pulses focused by 0.65-NA micro-objective as a function of pulse energy, exposure and inter-layer separation. The resulting microbits were visualized by 3D-scanning confocal Raman/photoluminescence microscopy as conglomerates of photo-induced quasi-molecular color centers and tested regarding their annealing. Minimal lateral and longitudinal microbit separations, enabling their robust read-out, were measured in LiF as 1.5 and 13 microns, respectively, to be improved regarding information storage capacity by more elaborate focusing systems. These findings pave a way to novel optical storage platforms utilizing ultrashort-pulse laser inscription of photoluminescent microbits as carriers of archival memory.

Keywords: fluorides; diamond; ultrashort-pulse laser; direct laser inscription; photoluminescent microbits; vacancy clusters

1. Introduction

Photoluminescence (PL) is one of the most important optical processes, underlying relaxation of two-level quasi-molecular systems upon their complementary optical excitation [1]. Even single PL photons could be acquired and spatially resolved much easier than differential absorption of single photons. As a result, PL characterization in 2D- or 3D-scanning confocal micro- or nano-spectroscopy mode became an enabling tool for probing local molecular or crystalline structures [2,3], or electromagnetic near-fields [4,5].

(Sub)microscale laser modification of molecular or crystalline structures and related PL spectra underlies facile and robust encoding of bulk diamonds for their tracing applications in identifying synthetic diamonds between natural ones in large commercial diamond collections [6], protecting trademarks of high-quality natural (potentially, synthetic too) diamond manufacturers [7], limiting commercial trading and marketing of illegal diamonds. This PL-based encoding appears unique in diamonds, where other popular encoding technologies – ablation fabrication of (sub)microscale voids [8] or birefringent nanogratings [9,10] – don't work in the ultra-hard diamond lattice, better tending to graphitization [11], while PL read-out is more simple and sensitive. Similarly, many other crystalline scintillators and luminophores undergo laser modification of their crystalline structures and related PL spectra [12-14], potentially promising for optical encoding (writing/read-out) applications in storage devices.

In this work we report an evaluation study of natural diamond, LiF and CaF_2 crystals as optical platforms for microscale photoluminescent encoding by ultrashort-pulse lasers for archival optical storage, their tests of potential capacity and viability.

2. Materials and Methods

In these studies, a 2-mm thick colorless brick of IaA-type natural diamond (total concentration of nitrogen atoms ≈130 ppm), and 5-mm thick slabs of undoped LiF and CaF_2 crystals grown by Bridgman-Stockbarger method were utilized, being optically transparent at the writing laser

Preprints (www.preprints.org) | NOT PEER-REVIEWED | Posted: 11 May 2023 doi:10.20944/preprints202305.0799.v1

wavelength of 525 nm (Figure 1a). The samples were characterized in the spectral range of 350–750 nm by room-temperature (RT) optical transmission microspectroscopy (Figure1b), using an ultraviolet(UV)−near-IR microscope-spectrometer MFUK (LOMO, Saint-Petersburg, Russia). Inscription inside these bulk crystals at the depth of 100 μm (fluorides) and of 120 μm (diamond) in their transparency spectral region (Figure 1b), accounting for their 525-nm refractive indexes of 2.4 (diamond), 1.4 (LiF) and 1.4 (CaF_2) [15], was performed by second-harmonic (525 nm) pulses of the Yb-crystal laser TEMA (Avesta Project, Moscow, Russia) with the pulsewidth (full width at a half maximum) of 0.2 ps, repetition rate of 80 MHz cut in pulse bunches of 0.05÷10-s duration by a mechanical shutter, and 50-nJ (average power – 4 W) maximum output pulse energy E in the TEM_{00} mode. The 525-nm laser pulses with variable energies $E \leq 50$ nJ were focused in a sub-filamentary regime (filamentation threshold energy ≈ 300 nJ (diamond), 260 nJ (CaF_2) [16]) by a 0.65-NA micro-objective into ≈1-μm wide spots (1/e-intensity diameter) inside the crystals, providing the peak laser fluence <6 J/cm² and peak laser intensity <30 TW/cm². The samples were mounted on a computer-driven three-dimensional motorized translation stage and exposed in separate position with variable transverse spacings in the range of 1-5 microns and longitudinal spacings in the range of 1-28 microns.

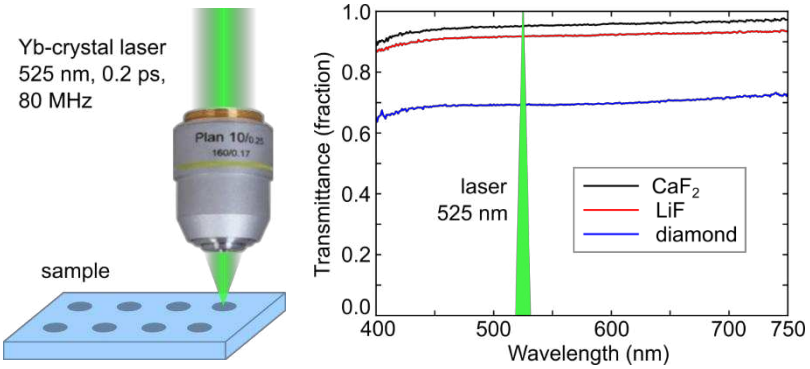

(**a**) (**b**)

Figure 1. (a) Laser inscription setup, sketching the PL-microbit inscription procedure; (b) transmittance spectra of natural diamond, LiF and CaF_2 crystals, with the laser writing wavelength of 525 nm shown in their transparency spectral region by the green triangle.

Annealing of fluoride samples was performed at different temperatures in the range of 25-300°C (20-min temperature ramp, 30 min – stationary heating), using a temperature-controlled mount for Raman micro-spectroscopy, while the diamond sample was annealed in an evacuated oven during 1 hour at different temperatures in the range of 25-1200°C.

In our characterization studies, top-view and side-view (cross-sectional) photoluminescence imaging at the 532-nm pump cw-laser wavelength and magnification 100x (NA = 1.45, spatial resolution ~1 μm) was performed by means of a 3D-scanning confocal photoluminescence/Raman microscope Confotec MR520 (SOL Instruments, Minsk, Belarus) to measure relative intensity, spatial dimensions and optical PL-acquired separation of PL microbits (Figure 2).

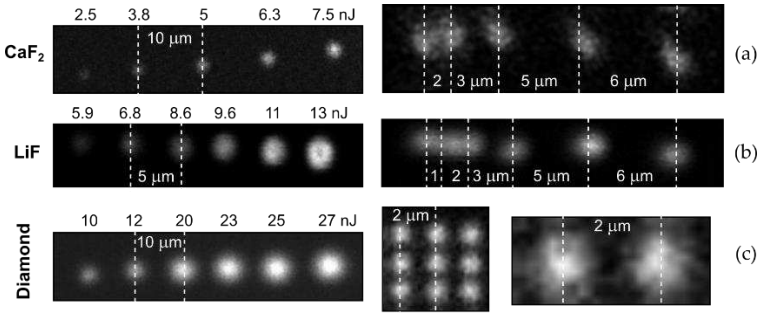

 doi:10.20944/preprints202305.0799.v1

Figure 2. (left) Top-view images of linear slices of square PL microbit arrays inscribed at different laser conditions in CaF_2 (a, PL image acquired at 755 nm), LiF (b, PL image acquired at 650 nm) and natural diamond (c, PL image acquired at 650 nm). (right) Their corresponding front-view images of neighboring PL microbits inscribed in these dielectrics at different transverse separations, varying in the range of 1-6 μm.

3. Experimental Results and Discussion

3.1. Inscription of Photo-Luminescent Microbits

PL microbits were inscribed in the bulk crystalline CaF_2 and LiF slabs, as well as in the diamond plate, at different pulse energies (Figure 2a-c, left side). Specifically, the PL microbits inside the CaF_2 slab exhibit the corresponding energy-dependent microbit dimensions above the inscription threshold value ≈3 nJ at the exposure of 10^7-10^9 pulses/microbit. Similarly, the PL microbits were inscribed inside the LiF slab in the same energy range, while the threshold energy appears considerably higher (≈ 5 nJ, Figure 2b, left side) at the exposure of 10^7-10^9 pulses/microbit, reflecting the higher bandgap energy of 13.0-14.2 eV in LiF [17,18], comparing to CaF_2 –11.5-11.8 eV [19,20]. Finally, in the diamond plate the PL microbits were inscribed as a function of laser pulse energy, demonstrating their increasing dimensions at the exposure of 10^7-10^9 pulses/microbit (Figure 2c, left side). Surprisingly, against our expectations, the inscribed microbits appear inhomogeneous at higher magnifications (Figure 2a-c, right side) because of well-known high degree of clustering – up to nanoscale - for fluorine atoms around dislocations in the fluoride crystals [21], while in diamonds such segregation of vacancies and interstitials also occurs in the form of multi-vacancies (voidities) [22] or interstitial aggregates in B2-centers [22]. In the same line, these microbits look diffuse owing to the low diffusion energies ~ 0.1 eV of interstitials and vacancies [21], facilitating room-temperature internal segregation and external collateral spreading of point-defect concentrations in the PL microbits.

In terms of spatial resolution of the PL microbits during the laser inscription process, even at low above-threshold pulse energies these features could be more or less resolved only at their 2-μm separation (Figure 2a-c, right side). The main reason of such moderate lateral (transverse) resolution is apparently the initial focal 1/e-diameter of 1 μm at the focusing NA = 0.65 (see Section 2 – Materials and Methods), additionally increased by ≈1-μm lateral diffusion length of fs-laser generated electron-hole plasma during its electron-lattice thermalization over the 1-2 picoseconds [23]. The corresponding point beam stability upon the focusing could result in negligible lateral displacements ~10 nm. As a result, distinct resolution of the neighboring PL microbits becomes possible for their lateral separations, exceeding 2-μm distance. Meanwhile, it could be considerably improved till ~1-1.5 μm, utilizing specially designed high-NA (0.75-0.9) air focusing micro-objectives. Below, in Section 3.4 the longitudinal (interlayer) spatial resolution will be tested in the case of brightly luminescent LiF crystal to evaluate the potential optical storage capacity of PL microbit arrays.

3.2. Photo-Luminescence Spectra of Microbits: Atomistic Inscription and Annealing Mechanisms

Typical PL spectra acquired in the laser-inscribed microbits by 3D-scanning confocal PL micro-spectroscopy are presented in Figure 3 in comparison to the corresponding spectra of the background non-modified materials. Specifically, the CaF_2 slab exhibits the strongly enhanced PL yield in the region of 650-850 nm, peaked at 740 nm (Figure 3a). Though PL spectra of electronic excitations in fluorides are rather flexible due to high mobility of Frenkel defects and the multitude of their complexes [21,24-25], the observed peak could be assigned to some of these vacancy aggregates ($F_x^{0,+}$, where F is the fluorine vacancy with the rapped electron, $x > 2$ and upper indexes "$^{0,+}$" denote the charged states). Similarly, in the LiF slab the increased PL band in the range of 550-750 nm could be assigned to F_2 (peak at 670 nm [24]) and F_3 (peak at 650 nm [24]) centers, while the emerging PL band with its peak at 800-850 nm could also related to some unknown yet $F_x^{0,+}$ centers [21,24-25].

Preprints (www.preprints.org) | NOT PEER-REVIEWED | Posted: 11 May 2023 doi:10.20944/preprints202305.0799.v1

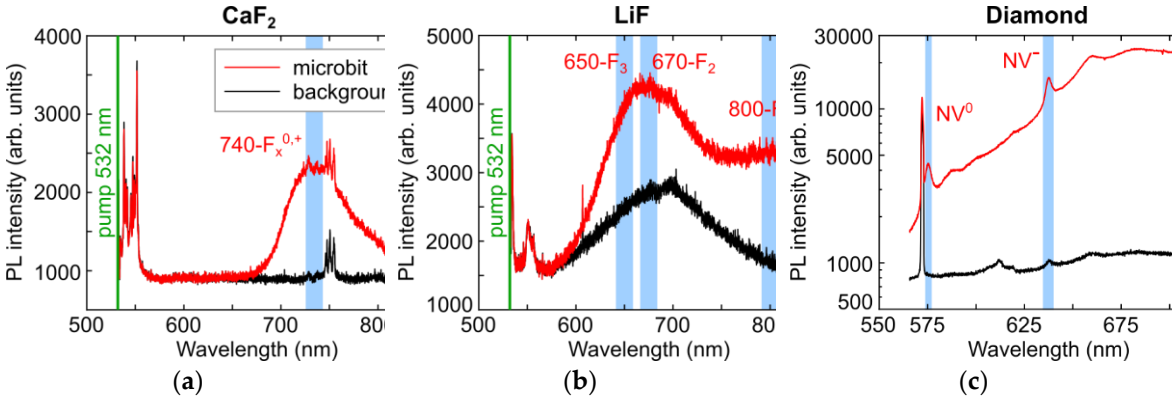

Figure 3. PL spectra of separate PL microbits (red curves) inscribed in CaF_2 (a), LiF (b) and natural diamond (c) regarding their background spectra of the unmodified materials (dark curves).

Finally, the observed strongly – by one order of magnitude - enhanced PL band in the micromark inscribed inside the diamond slab exhibits the main spectral features, representing the neutral (NV^0, zero-phonon line, ZPL, at 575 nm [22]) and negatively charged nitrogen-vacancy (NV^-, zero-phonon line at 637 nm [22]) centers of a substitutional nitrogen atoms with a photo-generated vacancy, as well as their red-shifted phonon replica.

Atomistic processes underlying the observed laser-induced transformations of PL spectra in LiF and CaF_2 are supposed to be associated with aggregation of mobile neutral (I-center [21]) and negatively charged (F-center [21]) vacancies, along with fluorine neutral (H-center [21]) and negatively charged (α-centers [21]) interstitials (Eq. 1a), approaching to hundreds of aggregated defects usually concentrated in dislocation loops [21]. Likewise, in the diamond plate the mobile photo-generated vacancies could be trapped by substitutional nitrogen atoms (C-centers [22]), resulting in well-known neutral or charged NV complexes [12,22] (Eq. 1b):

$$florides:\ H + H \rightarrow H_2, H + V_K \rightarrow F_3^-, \tag{1a}$$

$$diamond:\ N_S + V^0 \rightarrow NV\,. \tag{1b}$$

Equation 1. Atomistic processes, resulting in photo-induced vacancy complexes in fluorides and diamond.

In the same line, one can see strong stationary annealing of mobile vacancy-related color centers in LiF already at temperatures, elevated by 200-300°C (Figure 4a), almost deleting the microbit signal. In contrast, in denser and more rigid diamond lattice the Frenkel vacancies anchored by C-centers, remain rather stable even at high temperatures, approaching to 1200°C (Figure 4b).

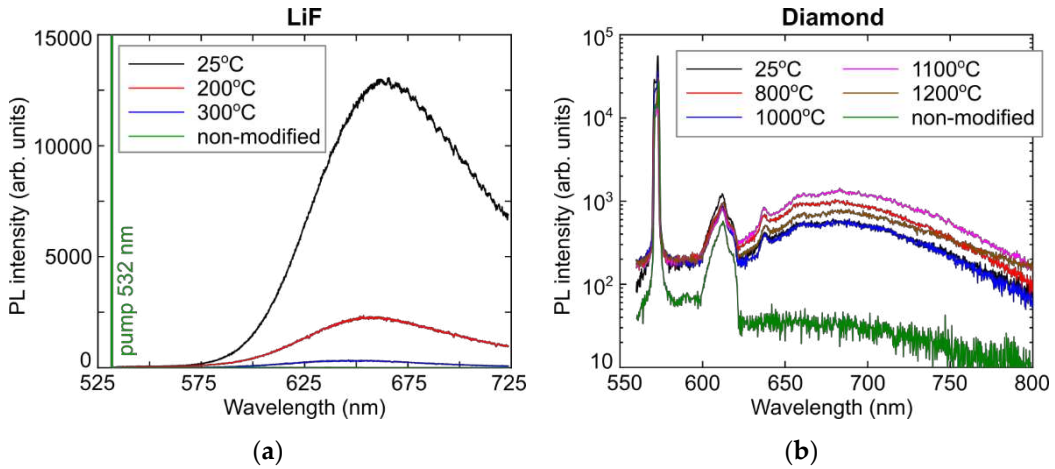

Preprints (www.preprints.org) | NOT PEER-REVIEWED | Posted: 11 May 2023 doi:10.20944/preprints202305.0799.v1

Figure 4. PL spectra of LiF (a) and natural diamond (b) upon annealing in the corresponding different temperature ranges, regarding the un-annealed non-modified materials.

3.3. Photogeneration of Frenkel Pairs of Point Defects in LiF during Atomistic Inscription

PL yield at 670 nm – in the peak related to F_2-centers – was used to track fs-laser photogeneration of Frenkel pairs in LiF, underlying the formation of these centers. As can be seen in Figure 5a,c, the PL yield in LiF exhibits the non-linear (power slope in the range of ≈ 3.3-3.8) monotonic dependence on pulse energy E = 2.5-13 nJ (peak fluence ≈ 0.3-1.7 J/cm², peak intensity ≈ 1.5-9 TW/cm²) (previously – in diamond [26]) and exposure of (4-800)×10⁶ pulses/spot (at room temperature, Figure 5b,d). Moreover, the abovementioned annealing effect at the temperatures of 200°C and 300°C results not only in the decreased PL intensity at 670 nm (Figure 5c), but also in the different exposure trends (Figure 5d) apparently related to cumulative heating of the material at the ultra-high 80-MHz exposure of the static sample, which is well-known to be favorable for self-trapped exciton stabilization via Frenkel pair formation [21]. The cumulative heating effect is more pronounced at the room temperature (Figure 5d), while the elevated temperatures make it less distinct.

We have analyzed the observed PL yield at 670 nm vs pulse energy E in LiF (Figure 5c), representing the concentration of F_2-centers in the probed confocal volume, alike to our previous similar studies in diamond [26]. According to high bandgap energy of $E_{dir}(\Gamma\text{-point}) \approx 13.0\text{-}14.2$ eV in LiF [17,18], formation of F_2-centers requires either $N = E_{dir}/\hbar\omega \approx 6$ photons at the 525 nm wavelength (photon energy $\hbar\omega \approx 2.4$ eV), or "hot" non-equilibrium electron of this energy (effectively, considerably higher to fulfill both the quasi-momentum and energy conservation laws). The evaluated laser-induced prompt ponderomotive enhancement of the bandgap [27,28], $U_P = e^2E^2/(4m_{opt}\omega^2)$, is minor (<1 eV) in the utilized intensity range of 9-30 TW/cm² (electric field strenth E=15-30 MV/cm) for the arbitrary optical mass of electron-hole pair $m_{opt} = m_e m_h/(m_e+m_h) = m_0/2$, assuming $m_e, m_h = m_0$ (free-electron mass).

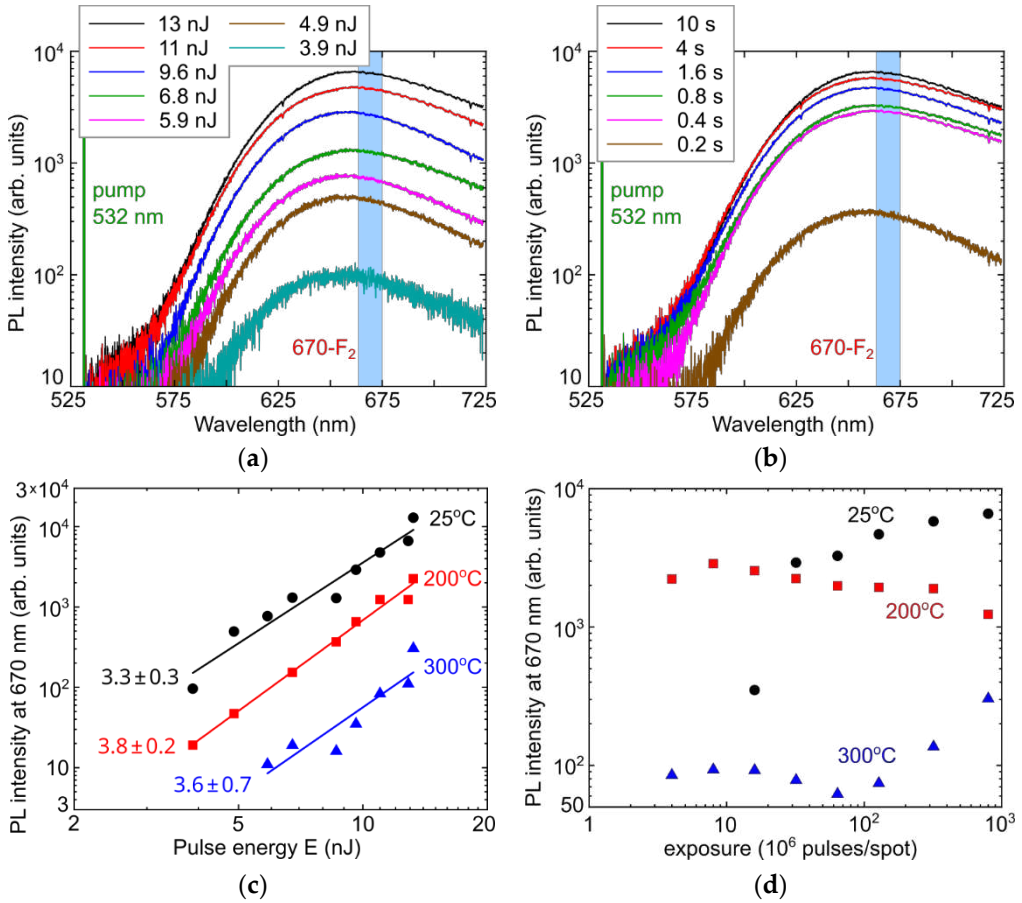

Preprints (www.preprints.org) | NOT PEER-REVIEWED | Posted: 11 May 2023 doi:10.20944/preprints202305.0799.v1

Figure 5. (a) PL spectra of microbits in LiF inscribed at the variable pulse energy (see the frame inset) and the fixed exposure of 10 s (×80 MHz), spectral assignment after [24]; (b) PL spectra of microbits in LiF inscribed at the variable exposures (see the frame inset) and the fixed pulse energy of 13 nJ (spectral assignment after [24]); (c) PL intensity of 670-nm (F_2-center [24]) peak in the spectra as a function of pulse energy (peak fluence – 0.2-2.4 J/cm^2, peak intensity – 1-12 TW/cm^2) at the maximal exposure of 10 s without annealing (25°C, black circles) and after annealing at 200°C (red squares) and 300°C (blue triangles) as well as their linear fitting curves of the same colors with the corresponding slopes; (d) PL intensity of 670-nm (F_2-center [24]) peak in the spectra as a function of exposure at the pulse energy of 13 nJ without annealing (25°C, black circles) and after annealing at 200°C (red squares) and 300°C (blue triangles).

Recently, for such analysis of electron-hole plasma and PL dynamics a kinetic rate model for electron-hole plasma density ρ_{eh} was enlighteningly used in the common form [29], including 1) ultrafast, pulsewidth-limited multiphoton (cross-section σ_N) and 2) impact ionization (coefficient α), 3) fast picosecond Auger (coefficient γ) and 4) slow radiative (coefficient β) recombination, as well as 5) fast self-trapping of electron-hole pairs (excitons, characteristic time τ_{str}) to produce one color center per self-trapped excitons [21] as the consecutive terms, respectively, and describing the corresponding continuous-wave-laser pumped PL yield Φ_{PL} as follows (Eq. 2a) [23]:

$$\frac{d\rho_{eh}}{dt} = \sigma_N I^N + \alpha I \rho_{eh} - \gamma \rho_{eh}^3 - \beta \rho_{eh}^2 - \frac{\rho_{eh}^2}{\tau_{str}}, \Phi \propto \int \rho_{eh}^2 dt \qquad (2a)$$

$$\frac{d\rho_{eh}}{dt} = \sigma_6 I^6 - \gamma \rho_{eh}^3 - \frac{\rho_{eh}^2}{\tau_{str}}, \sigma_6 I^6 \approx \gamma \rho_{eh}^3, \rho_{eh} \propto I_0^2, \Phi \propto \int \rho_{eh}^2 dt \propto I_0^4. \qquad (2b)$$

Equation 2. Kinetic rate equations for electron-hole plasma and related PL yield Φ_{PL} of the F_2-centers produced via exciton self-trapping [21]: (a) general form, (b) case-specific form for our experiments in LiF.

In the case of LiF, Equation 2a could be presented in the case - specific form (Eq. 2b), where the only six-photon ionization and Auger recombination balance each other, while excitonic self-trapping accompanies the electron-hole plasma relaxation. As a result, PL yield could follow the non-linear dependence on I_0 with the power slope ≈ 4, being consistent with the measured values of 3.3-3.8 (Figure 5c).

3.4. Evaluation of Storage Capacity of Photo-Luminescent Microbits

Finally, we have performed experimental evaluation of PL microbit density, which is the key characteristic of archival optical storage. Above, we have inscribed PL bits in the natural diamond, LIF and CaF_2 samples with ≥2-μm lateral separation, which could be easily resolved in PL images (Figure 2). Furthermore, we have undertaken inscription and confocal PL visualization of separate linear arrays of PL microbits with variable vertical (depth) separation, changing in the range of 1-28 μm (Figure 6), in order to evaluate the minimal resolvable vertical separation. PL visualization was performed by means of Olympus (40x) and Nikon (100x) microscope objectives with vertical resolution Δz = 1 or 2 μm, respectively (Figure 6a,b). The corresponding side-view PL imaging results for the same microstructure of paired linear arrays are presented in Figure 6c,d.

Preprints (www.preprints.org) | NOT PEER-REVIEWED | Posted: 11 May 2023 doi:10.20944/preprints202305.0799.v1

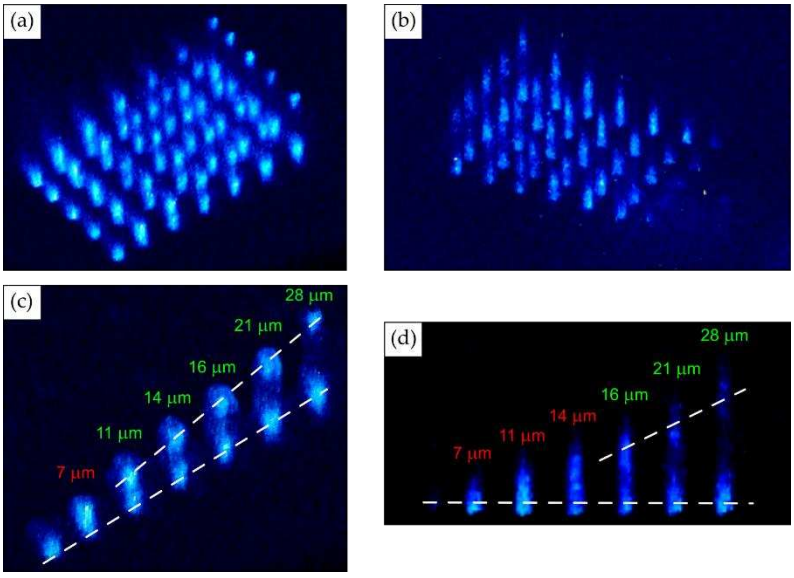

Figure 6. PL imaging of stair-like set of pairs of linear microbit arrays in LiF with variable intra-pair vertical separation in the range of 1-28 μm using Olympus (a,c) and Nikon (b,d) microscope objectives with the vertical resolution Δz = 1 or 2 μm, respectively: (a,b) 3D view; (c,d) side-view images of neighboring PL microbit arrays, showing their resolvable separation, starting from 11 μm (c) or 16 μm (d).

Here, one can find that the pairs of the microbit lines become visibly separable, staring from 11 μm for the 1μm-resolution visualization (Figure 6c), while only at 16 or 21 μm – for the 2μm-resolution visualization (Figure 6d). Hence, accounting for the appropriately resolvable 2-μm intra-layer separation of microbits and their 11-μm inter-layer separation, one can evaluate for the simple cubic lattice of microbits the bulk microbit density of 25 Gbits per cubic centimeter, i.e., about 3 Tbits per disk for the 120-mm diameter of the standard CV or DVD disks and the 10-mm thickness. This optical storage capacity is comparable to previous optical memory writing technologies (visible microvoids [8], birefringent nanotrenches [9,10], photoluminescent microbits [30]), but have clear benefits in the confocal non-linear memory read-out due to non-destructive laser inscription technology. Moreover, considerable, few-fold additional increase in the storage capacity could be achieved by higher-NA (NA > 0.65) inscription and other advanced optical means.

4. Conclusions

In this study, bulk high-NA inscription (writing) of photo-luminescent microbits in LiF, CaF_2 and diamond crystals was performed by means of ultrashort-pulse laser and tested (read-out) by 3D-scanning confocal photoluminescence micro-spectroscopy. Preliminarily, optical storage density for the simple cubic lattice of microbits was evaluated as high as 25 Gbits/cm^3, but could be few-fold increased by using more sophisticated optical focusing tools. Photo-luminescent color centers were identified in the fluorides (fluorine vacancy-based F_2-centers) and diamond (carbon vacancy-based NV-centers) by the PL micro-spectroscopy, while their laser inscription mechanism was revealed in fluorides for the first time, comparing to the know mechanism for synthetic diamonds. Moreover, the color centers could be easily annealed in the fluorides at moderate temperatures of 300°C due to the high lability of the centers and room-temperature mobility of their atomistic constituents, comparing to the relatively robust color (NV) centers in the diamond, persisting even at rather elevated temperatures ≈1200°C. Our research paves the way for potential implications of laser-inscribed photo-luminescent microbits in archival optical storage.

Author Contributions: Conceptualization, S.K., P.D. and A.G.; methodology, I.M.; validation, E.K.; investigation, A.R., P.D., N.S. and E.K.; resources, A.R., G.K. and R.K.; writing—original draft preparation, S.K.; writing—review and editing, A.G. and S.K.; visualization, P.D., E.K. and N.S.; supervision, A.G.; project

administration, S.K.; and funding acquisition, S.K. All authors have read and agreed to the published version of the manuscript.

Funding: This research was funded by the Russian Science Foundation (project no. 21-79-30063); https://rscf.ru/en/project/21-79-30063/.

Data Availability Statement: The data supporting the reported results are presented in part in Supplementary data and can be also obtained from the authors.

Conflicts of Interest: The authors declare no conflict of interest.

References

1. Levshin, L.; Saletskii, A. Optical Methods for Studying Molecular Systems. Molecular Spectroscopy; MGU: Moscow, Russia, 1994.
2. Yang, B.; Chen, G.; Ghafoor, A.; Zhang, Y.; Zhang, Y.; Zhang, Y.; ... Hou, J. G. Sub-nanometre resolution in single-molecule photoluminescence imaging. *Nature Photonics* **2020**, *14*(11), 693-699.
3. Goldschmidt, J. C.; Fischer, S. Upconversion for photovoltaics–a review of materials, devices and concepts for performance enhancement. *Advanced Optical Materials* **2015**, *3*(4), 510-535.
4. Kudryashov, S.I.; Danilov, P.A.; Porfirev, A.P.; Saraeva, I.N.; Kuchmizhak, A.A.; Rudenko, A. A.; Busleev, N.I.; Umanskaya, S.F.; Zayarny, D.A.; Ionin, A.A.; Khonina, S.N. Symmetry-wise nanopatterning and plasmonic excitation of gold nanostructures by structured femtosecond laser pulses, *Optics Letters* **2019**, 44 (5), 1129-1132.
5. Zhizhchenko, A. Y.; Tonkaev, P.; Gets, D.; Larin, A.; Zuev, D.; Starikov, S.; ... Makarov, S. V. Light-emitting nanophotonic designs enabled by ultrafast laser processing of halide perovskites. *Small* **2020**, *16*(19), 2000410.
6. Tsai, T. H. Imaging-assisted Raman and photoluminescence spectroscopy for diamond jewelry identification and evaluation. *Applied Optics* **2023**, *62*(10), 2587-2594.
7. ALROSA. Identification of diamonds using laser nanomarks. Available online: https://youtu.be/X3Z_jcWowks (accessed on 11 December 2022).
8. Hong, M. H.; Luk'yanchuk, B.; Huang, S. M.; Ong, T. S.; Van, L. H.; Chong, T. C. Femtosecond laser application for high capacity optical data storage. *Applied Physics A* **2004**, *79*, 791-794.
9. Wang, H.; Lei, Y.; Wang, L.; Sakakura, M., Yu, Y.; Shayeganrad, G.; Kazansky, P.G. 100-Layer Error-Free 5D Optical Data Storage by Ultrafast Laser Nanostructuring in Glass. *Laser & Photonics Reviews* **2022,** 16(4), 2100563.
10. Lipatiev, A. S.; Fedotov, S. S.; Lotarev, S. V.; Lipateva, T. O.; Shakhgildyan, G. Y.; Sigaev, V. N. Single-Pulse Laser-Induced Ag Nanoclustering in Silver-Doped Glass for High-Density 3D-Rewritable Optical Data Storage. *ACS Applied Nano Materials* **2022**, *5*(5), 6750-6756.
11. Ionin, A.A.; Kudryashov, S.I.; Mikhin, K.E.; Seleznev, L.V.; Sinitsyn, D.V. Bulk femtosecond laser marking of natural diamonds. *Laser Phys.* **2010**, *20*, 1778–1782.
12. Chen, Y.C.; Salter, P.S.; Knauer, S.; Weng, L.; Frangeskou, A.C.; Stephen, C.J.; Ishmael, S.N.; Dolan, P.R.; Johnson, S.; Green, B.L.; Morley, G.W.; Newton, M.E.; Rarity, J.G.; Booth, M.J.; Smith, J.M. Laser writing of coherent colour centres in diamond. *Nat. Photonics* **2017**, *11*, 77–80.
13. Chekalin, S. V.; Kompanets, V. O.; Dormidonov, A. E.; Kandidov, V. P. Influence of induced colour centres on the frequency–angular spectrum of a light bullet of mid-IR radiation in lithium fluoride. *Quantum Electronics* **2017**, *47*(3), 259.
14. Castelletto, S.; Maksimovic, J.; Katkus, T.; Ohshima, T.; Johnson, B.C.; Juodkazis, S. Color centers enabled by direct femtosecond laser writing in wide bandgap semiconductors. *Nanomaterials* **2020**, 11(1), 72.
15. Palik, E.D. *Handbook of Optical Constants of Solids*; Academic Press: Orlando, USA, 1998.
16. Kudryashov, S. I.; Danilov, P. A.; Kuzmin, E. V.; Gulina, Y. S.; Rupasov, A. E.; Krasin, G. K.; ... Ionin, A. A. Pulse-width-dependent critical power for self-focusing of ultrashort laser pulses in bulk dielectrics. *Optics Letters* **2022**, 47(14), 3487-3490.
17. Samarin, S.; Artamonov, O. M.; Suvorova, A. A.; Sergeant, A. D.; Williams, J. F. Measurements of insulator band parameters using combination of single-electron and two-electron spectroscopy. *Solid state communications* **2004**, *129*(6), 389-393.
18. Karsai, F.; Tiwald, P.; Laskowski, R.; Tran, F.; Koller, D.; Gräfe, S.; Blaha, P. F center in lithium fluoride revisited: Comparison of solid-state physics and quantum-chemistry approaches. *Physical Review B* **2014**, *89*(12), 125429.
19. Ma, Y.; Rohlfing, M. Quasiparticle band structure and optical spectrum of CaF2. *Physical Review B* **2007**, *75*(20), 205114.
20. Chen, J.; Zhang, Z.; Guo, Y.; Robertson, J. Electronic properties of CaF2 bulk and interfaces. *Journal of Applied Physics* **2022**, *131*(21), 215302.
21. Song, K.; Williams, R.T. *Self-trapped excitons*; Springer-Verlag Berlin: Heidelberg, Germany, 1993.

22. Zaitsev, A. M. *Optical properties of diamond: a data handbook;* Springer-Verlag Berlin, Heidelberg, Germany, 2001.
23. Kudryashov, S.; Danilov, P.; Smirnov, N.; Krasin, G.; Khmelnitskii, R.; Kovalchuk, O.; ... Levchenko, A. "Stealth Scripts": Ultrashort Pulse Laser Luminescent Microscale Encoding of Bulk Diamonds via Ultrafast Multi-Scale Atomistic Structural Transformations. *Nanomaterials* **2023**, 13(1), 192.
24. Lakshmanan, A. R.; Madhusoodanan, U.; Natarajan, A.; Panigrahi, B. S. Photoluminescence of F-aggregate centers in thermal neutron irradiated LiF TLD-100 single crystals. *Physica status solidi (a)* **1996**; *153*(1), 265-273.
25. Davidson, A. T.; Kozakiewicz, A. G.; Comins, J. D. Photoluminescence and the thermal stability of color centers in γ-irradiated LiF and LiF (Mg). *Journal of applied physics* **1997**, *82*(8), 3722-3729.
26. Kudryashov, S.I.; Danilov, P.A.; Smirnov, N.A.; Stsepuro, N.G.; Rupasov, A.E.; Khmelnitskii, R.A.; Oleynichuk, E.A.; Kuzmin, E.V.; Levchenko, A.O.; Gulina, Y.S.; Shelygina, S.N.; Sozaev, I.V.; Kovalev, M.S.; Kovalchuk, O.E. Signatures of ultrafast electronic and atomistic dynamics in bulk photoluminescence of CVD and natural diamonds excited by ultrashort laser pulses of variable pulsewidth. *Appl. Surf. Sci.* **2021**, *575*, 151736.
27. Keldysh, L.V. Ionization in the field of a strong electromagnetic wave, *Sov. Phys. JETP* **1965**, *20*, 1307–1314.
28. Kudryashov, S.I. Microscopic model of electronic Kerr effect in strong electric fields of intense femtosecond laser pulses. In Proceedings of the Conference on Quantum Electronics and Laser Science, Baltimore, Maryland, USA, May 2005; JThE26.
29. Bulgakova, N.M.; Stoian, R.; Rosenfeld, A.; Hertel, I.V.; Campbell, E.E.B. Electronic transport and consequences for material removal in ultrafast pulsed laser ablation of materials. *Phys. Rev. B* **2004**, *69*, 054102.
30. Ren, Y.; Li, Y.; Guo, K.; Cui, Z.; Wang, C.; Tan, Y.; ... Cai, Y. Dual-modulation of micro-photoluminescence in rare-earth-doped crystals by femtosecond laser irradiation for 5D optical data storage. *Optics and Lasers in Engineering* **2023**, *167*, 107612.